

Calibration of Ground Pressure on Tunnel Lining in Genetic Algorithm Application for Structural Monitoring

*Original*

Calibration of Ground Pressure on Tunnel Lining in Genetic Algorithm Application for Structural Monitoring / Cortese, Giuseppe; Bertagnoli, Gabriele. - In: IOP CONFERENCE SERIES: MATERIALS SCIENCE AND ENGINEERING. - ISSN 1757-899X. - ELETTRONICO. - 960:(2020), p. 022096. ( 5th World Multidisciplinary Civil Engineering-Architecture-Urban Planning Symposium – WMCAUS 15-19 June 2020, Prague, Czech Republic Prague 15-19 June 2020) [10.1088/1757-899X/960/2/022096].

*Availability:*

This version is available at: 11583/2857078 since: 2020-12-12T10:25:10Z

*Publisher:*

IOP Publishing

*Published*

DOI:10.1088/1757-899X/960/2/022096

*Terms of use:*

This article is made available under terms and conditions as specified in the corresponding bibliographic description in the repository

*Publisher copyright*

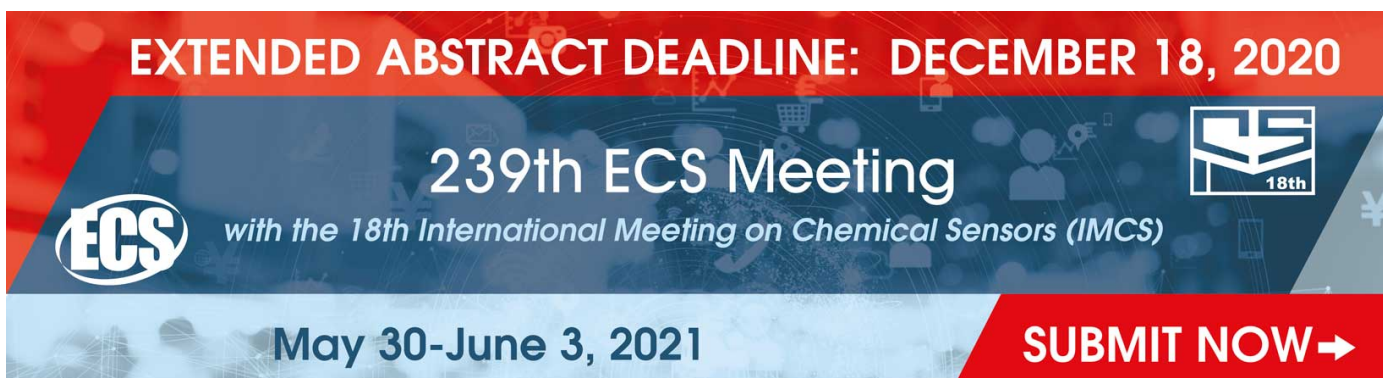
(Article begins on next page)

PAPER • OPEN ACCESS

## Calibration of Ground Pressure on Tunnel Lining in Genetic Algorithm Application for Structural Monitoring

To cite this article: Giuseppe Cortese and Gabriele Bertagnoli 2020 *IOP Conf. Ser.: Mater. Sci. Eng.* **960** 022096

View the [article online](#) for updates and enhancements.



**EXTENDED ABSTRACT DEADLINE: DECEMBER 18, 2020**

**239th ECS Meeting**  
with the 18th International Meeting on Chemical Sensors (IMCS)

**May 30-June 3, 2021**

**SUBMIT NOW →**

The banner features a red top section with the deadline text, a dark blue middle section with the meeting title and logos, and a light blue bottom section with the dates. A red button with a white arrow is on the right.

# Calibration of Ground Pressure on Tunnel Lining in Genetic Algorithm Application for Structural Monitoring

Giuseppe Cortese<sup>1</sup>, Gabriele Bertagnoli<sup>1</sup>

<sup>1</sup> Dipartimento di Ingegneria Strutturale, Edile e Geotecnica, Politecnico di Torino (PoliTo), Corso duca degli Abruzzi, 24, 10129 Turin, Italy

gabriele.bertagnoli@polito.it

**Abstract.** This article presents the evolution of an algorithm that can be applied to a diagnostic systems for tunnels developed by the same authors. The aim of this work is the analysis of typical ground trust shape functions to be introduced in the library of a genetic algorithm in order to calculate the forces acting on tunnel lining starting only from the quantities measured by a set of clinometers and pressure sensors placed inside the lining itself, without any other knowledge of geotechnical or geological parameters. The knowledge of proper trust shapes, derived from geotechnical simulations, increases the performance of the algorithm in terms of convergence and correctness of the result. Some benchmarks of the genetic algorithm applied on geotechnical f.e.m. results is also given.

## 1. Introduction

The realization of underground structures is today more common than in the past within the construction of modern infrastructures for road and railway transport. Tunnel excavation has positive effects on the protection of landscape and traffic noise reduction, but it is nevertheless a procedure that faces many unknowns, because of the high variability of geological and geotechnical parameters that may be found during the realization. Monitoring of tunnels during excavation is today a standard approach [1] [2], but structural health monitoring (SHM) of these structures throughout the complete service life is not a widespread technique. During the last years, the evolution of low cost sensors, the development of high-speed internet communication, the birth of cloud based services and the rise of big data platforms, have changed the possible applications of structural monitoring [3] that can now be deployed on large scale to infrastructures.

This article presents the evolution of an algorithm that can be applied to a diagnostic systems for tunnels developed by the same authors. The aim of this work is the analysis of typical ground trust shape functions to be introduced in the library of a genetic algorithm developed by the same authors [4] in order to calculate the forces acting on tunnel lining starting only from the quantities measured by a set of clinometers and pressure sensors [5] placed inside the lining itself, without any other knowledge of geotechnical or geological parameters. The knowledge of proper trust shapes, derived from geotechnical simulations, increases the performance of the algorithm in terms of convergence and correctness of the result. Some benchmarks of the genetic algorithm applied on geotechnical f.e.m. results is also given.

The work described in this paper is based on the installation of an innovative monitoring system inside the tunnel lining [4]. The installation procedure is optimized for prefabricated segmental lining system where it is done in factory during the prefabrication of the segments, but can also be realized during the construction of the concrete lining if traditional excavation is used.



The monitoring system is based on a set of MEMS inclinometers and pressure sensors. Each ring section can be equipped by a high number of sensors as their cost is much lower than traditional laboratory instruments. The clinometers measure the rotation of the lining due to transverse ovalization, whereas the pressure sensors placed inside concrete can measure both axial force and bending moment as more than two of them are placed within the thickness of the concrete wall.

## 2. Genetic algorithm description

The genetic algorithm used in this paper is based on the former works of one of the authors [6], [7], [8]. The aim of the genetic algorithm is to calculate a set of radial and tangential pressures that applied to the lining from the ground, will reproduce the same rotations, and internal actions measured by the sensors. This set of pressures is then used to calculate internal actions along the lining cross section providing the best interpolation between the values measured by the sensors.

Internal actions inside a generic structure are in equilibrium with external loads and represent a minimum internal elastic energy condition for the structure. It is therefore better calculate internal actions starting from external loads than using interpolation techniques between measured points, as these techniques may find solutions that are not associated to minimum energy and are therefore more demanding and stressing for the structure than the real condition.

The population of the algorithm is represented by the radial and tangential actions that the terrain exchanges with the lining. This set of loads is divided into a hydrostatic part, which is the mean radial pressure associated to the depth of the centre of the lining from the surface, and a deviatoric part. The deviatoric part, which is responsible of rotation and ovalization, can be described by simple harmonic shape functions.

## 3. Tunnel characteristics and construction phases

A set of geotechnical analyses has been done using two commercial softwares: Flac 2D [6] and RS2 [7]. The two softwares use different theoretical approaches but demonstrated to give very similar results within the application field tested in this work.

At the beginning three deep tunnels in different conditions have been studied to calibrate the models using simple boundary conditions. In a second step a larger set of shallow tunnels has been studied.

In all models a circular tunnel with a diameter of 13.7m has been considered. The lining is modelled with 72 beam elements each of them covering  $5^\circ$  of angle at centre. The thickness of the lining is constant for all the analyses and equal to 0.70m. The lining is realized in concrete, which is supposed to be linear elastic material with the following properties: Young modulus  $E_c= 40$  GPa and Poisson coefficient  $\nu=0.2$ .

The construction phases are modelled following three phases:

1. Initial geostatic condition: the ground is in its not disturbed condition before the excavation
2. Tunnel section excavation and relative stress release equal to 60%. The ground within the excavation boundary is removed and a fictitious arrangement of forces on the boundary is placed to simulate 40% of geostatic action present on the boundary.
3. Lining installation and subsequent removal of the forces arrangement described at point 2; 40% of geostatic forces are transferred to the lining.

## 4. Deep tunnels

The model used for these analyses is squared with sides measuring 425x425 m. The ground is modelled as a linear elastic material. The mechanical properties of the ground are given in Table 1.

The stresses  $\sigma_1$  and  $\sigma_3$  are the principal ones in the plane of the section of the tunnel, whereas the stress  $\sigma_z$  is the out of the plane stress according to the plain strain hypothesis (nil strain in the direction of the tunnel axis). The angle  $\theta$  represents the inclination of the stress  $\sigma_1$  with respect to the horizontal (i.e.  $\theta=90^\circ$  means  $\sigma_1$  is vertical).

**Table 1.** Input data for deep tunnels.

Tunnel ID	Ground properties		Geostatic stress state			
	Eg [MPa]	$\nu$ [-]	$\sigma_1$ [MPa]	$\sigma_3$ [MPa]	$\sigma_z$ [MPa]	$\theta$ [°]
<b>D1</b>	6000	0.3	25	12.5	11.25	90°
<b>D2</b>	25000	0.2	25.74	6.14	6.376	75°
<b>D3</b>	3500	0.3	25	12.5	11.25	0°

### 5. Shallow tunnels

The analysis of shallow tunnels has been performed considering six ground typologies taken from the Itaca [8] database of INGV (Italian National Institute of Geophysics and Volcanos Science), three inclinations,  $i$ , of the ground level respect to the horizontal (0°, 10°, 20°) and three depths  $d$  of the tunnel: two, three and four times the diameter (2D, 3D, 4D).

The ground properties for each ground are presented in Table 2. A brief stratigraphy, the classification according to Eurocode EN 1992-8 [9] and the variation of the elastic modulus in function of the depth (in meters) from the ground level are provided. The modulus of elasticity has been derived by means of shear wave velocity correlation as shown in equations (1) and (2).

$$G [Pa] = \rho * V_s^2 \left[ \frac{kg}{m^3} * \frac{m^2}{s^2} \right] \quad (1)$$

$$E [Pa] = 2 * G * (1 + \nu) \quad (2)$$

The irregular profile of E obtained by field test has then been linearized to simplify the calculations: Table 2 presents the linearized simplification.

**Table 2.** Input data for ground of shallow tunnels.

Soil ID	Stratigraphy	Ground category EN 1992-8	Eg [MPa]
<b>1</b>	Brown cemented sands of the upper Pliocene.	B	$E(z) = 1000 + 57.5 * z$
	Silt with clay and silt with sandstone from upper Miocene.		
<b>2</b>	Recent alluvial deposit	D	$E(z) = 95 + 4.4 * z$
	Silt, clayey silt, peaty silt		
	Clay, silty clay, lake silt.		
	Neritic sediments (carbonate) Bedrock: limestone		
<b>3</b>	Lime soil, marly lime soil	C	$E(z) = 200 + 34 * z$
	Micritic lime soil		
	Bedrock: micritic limestone		
<b>4</b>	Recent alluvial deposit, gravel and sand over clay soil	B	$E(z) = 500 + 48 * z$
<b>5</b>	Backfilled soil	B	$E(z) = 185 + 130,3 * z$
	Silty sand		
	Silty gravel, silty gravel and sand		
	Silty sand		
	Clayey silt (low plasticity)		
<b>6</b>	Rock	B	$E(z) = 2466 + 64,5 * z$
<b>6</b>	Silty gravel with sand	B	$E(z) = 2466 + 64,5 * z$
	Silty very fine sand		
	Clayey silt (low plasticity)		

A total of 54 numerical models of shallow tunnels has therefore been analysed. The output of the analyses are the diagrams of the stresses transferred from the ground to the lining. Two kind of stresses are considered: normal stresses,  $\sigma$ , (orthogonal to the external surface of the lining) and tangential stresses,  $\tau$  (in circumferential direction). The results are therefore 54 diagrams of  $\sigma$  stresses (called radial loads), shown in Figure 1, and 54 diagrams of  $\tau$  stresses (called tangential loads), shown in Figure 2.

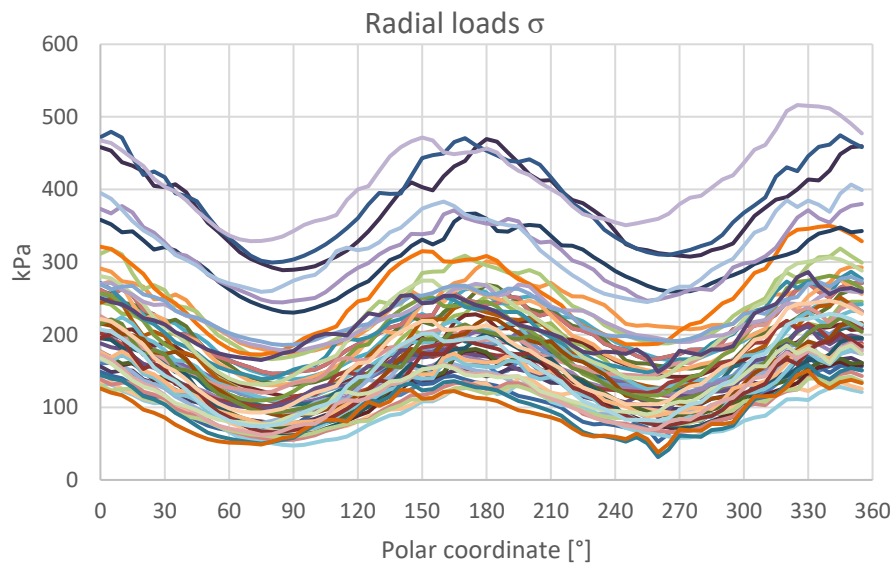


**Figure 1.** Radial stresses transmitted from the ground to the lining

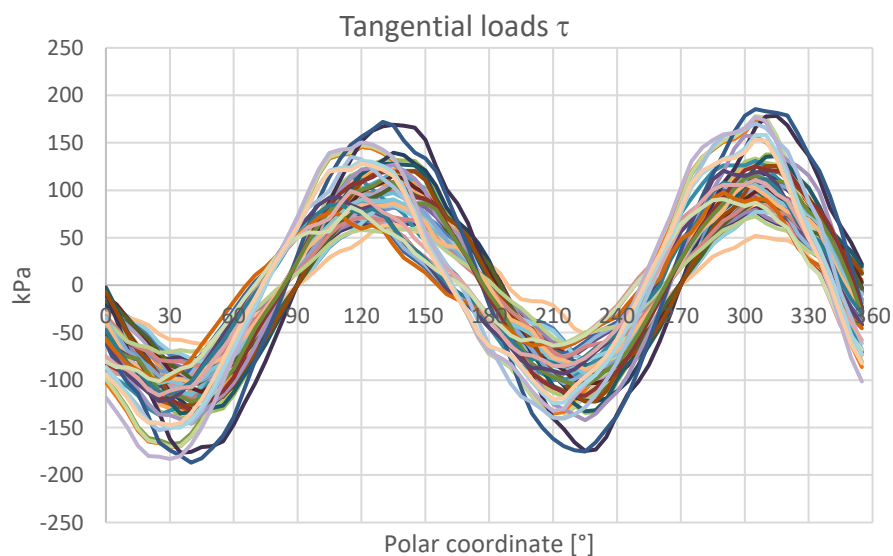


**Figure 2.** Tangential stresses transmitted from the ground to the lining

The stresses are presented along the lining using a polar coordinate shown in figure 3, where the zero is on the mountain side and the angles are counter clockwise. The depth  $d$  of the tunnel and the inclination  $i$  of the ground level are also shown in Figure 3.

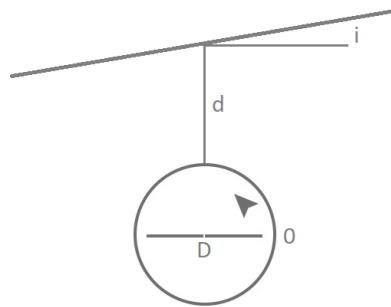


**Figure 3.** Polar referring system, depth  $d$  and diameter  $D$  of the tunnel and ground inclination

As it can be easily appreciated from the figures, the shape of the diagrams are all similar, for each family (radial or tangential). The main differences are the intensity of radial pressure (from 50 to 500 kPa) and some slight translation along the polar coordinate axis of the points where the pressure is maximum in function of the inclination of the ground level. Tangential stresses show smaller absolute value, as their maximum value is limited by axial load and friction coefficient.

### 6. Shape functions to be used in the genetic algorithm

Grounding on the results pictured in Figure 1 and 2 the following shape function for the ground thrust on the tunnel lining are proposed. Concentrated load components are eliminated and radial and tangential function are modified as follows:

Radial shape functions:

$$Ra: \quad \{\cos(\varphi + \theta_1)\} \cdot \alpha_a \quad (3)$$

$$Rb: \quad \{-\cos[2(\varphi + \theta_2)]\} \cdot \alpha_b \quad (4)$$

Tangential shape functions:

$$Ta: \quad \{\sin(\varphi + \theta_3)\} \cdot \beta_a \quad (5)$$

$$Tb: \quad \{\sin[2(\varphi + \theta_4)]\} \cdot \beta_b \quad (6)$$

Where:

- $\alpha_a$ ,  $\alpha_b$  are the maximum magnitude of harmonic radial loads, randomly generated from the genetic algorithm within a first interval given by the user in function of the depth of the tunnel and the expected characteristics of the ground;
- $\theta_1$ ,  $\theta_2$  are the phases of the harmonic radial loads;
- $\beta_a$ ,  $\beta_b$  are the maximum magnitude of harmonic tangential loads, randomly generated from the genetic algorithm within a second interval given by the user in function of the depth of the tunnel and the expected characteristics of the ground;
- $\theta_3$ ,  $\theta_4$  are the phases of the harmonic radial loads.

The meaning and the procedure to assign the values described above is explained in the following;  $Ra$  and  $Rb$  are added together and  $Ta$  and  $Tb$  are added together.

Radial shape function  $Rb$  is the one that gives the main shape to the radial load, whereas shape function  $Ra$  provides some modulation to  $Rb$  giving the opportunity to  $Rb$  of having different peak values as shown in Figure 4 for the shallow tunnel with horizontal ground surface, depth equal 2 times the diameter and soil ID 1. The magnitude of shape function  $Rb$  is chosen by the algorithm in the interval given by expression (7) where  $Ab$  is provided by the user

$$\alpha_b \in [0 ; A_b] \quad \text{where} \quad A_b > 0 \tag{7}$$

The magnitude of shape function  $Ra$  is chosen by the algorithm in the interval given by expression (8).

$$\alpha_a \in [-A_a ; A_a] \quad \text{where} \quad 0 < A_a < 0,3 \cdot A_b \tag{8}$$

Therefore the maximum difference between the peaks of  $Ra + Rb$  is 30% of the amplitude of  $Rb$ .

Tangential shape function  $Tb$  is the one that gives the main shape to the tangential load, whereas shape function  $Ta$  provides some modulation to  $Tb$  like seen for  $Ra$  and  $Rb$ . The magnitude of shape function  $Tb$  is chosen by the algorithm in the interval given by expression (9) where  $Bb$  is provided by the user

$$\beta_b \in [0 ; B_b] \quad \text{where} \quad B_b > 0 \tag{9}$$

The magnitude of shape function  $Ta$  is chosen by the algorithm in the interval given by expression (10).

$$\beta_a \in [-B_a ; B_a] \quad \text{where} \quad 0 < B_a < 0,1 \cdot B_b \tag{10}$$

The phases  $\theta_1, \theta_2, \theta_3, \theta_4$  are chosen by the genetic algorithm within an interval of  $\pm 30^\circ$  from the most probable inclination of the thrust of the ground  $\theta_p$  chosen by the user mainly in function of the inclination of the ground level, as shown in expression (11)

$$\theta_i \in [\theta_p - 30^\circ ; \theta_p + 30^\circ] \cup [(180^\circ + \theta_p) - 30^\circ ; (180^\circ + \theta_p) + 30^\circ] \tag{11}$$

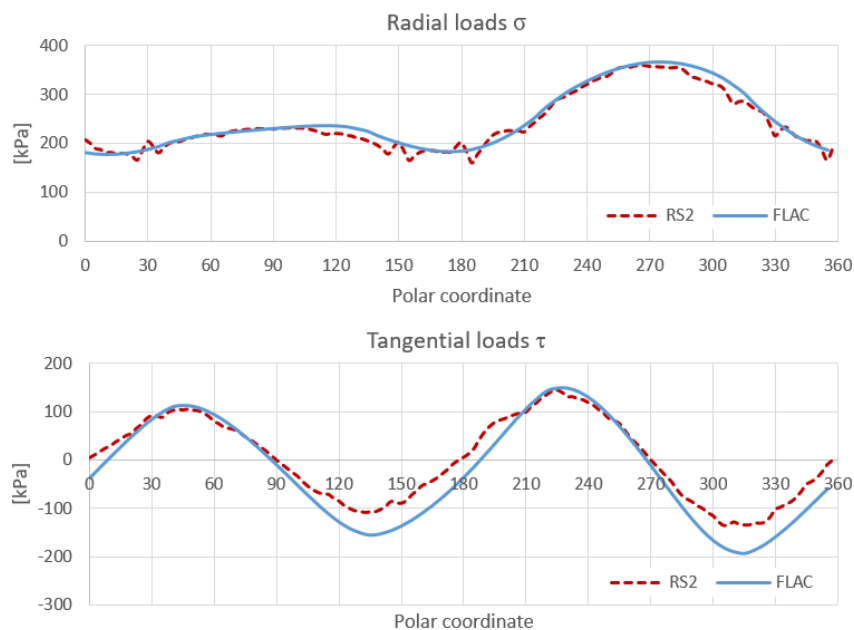


**Figure 4.** Comparison between RS2 and Flac lining loads for a given tunnel

As a conclusion the user has to provide to the algorithm the following input values:

- $q_{m,R}$ , mean radial pressure value which mainly depends on the depth of the tunnel.
- $A_b$ , maximum amplitude of the variation of the radial load.
- $B_b$ , maximum amplitude of the variation of the tangential load which is responsible of the variation of the axial force in the lining,
- $\theta_p$  which identifies the most probable ovalization direction
- $n$ , number of individuals of the population

## 7. Results of the application of the genetic algorithm to a deep and a shallow tunnel

In this paragraph are presented the results of the application of the genetic algorithm to two very different tunnels: a deep one, called D1, and a shallow one, characterized by a ground level inclination of  $10^\circ$ , depth of the tunnel equal to 2 diameters, and soil type 5 (see Table 2) and called PC10\_2D\_L5.

The user provided input parameters for both cases are resumed in Table 3.

**Table 3.** User provided input parameters in the genetic algorithm.

Tunnel ID	$q_{m,R}$ [kPa]	$\theta_p$ [ $^\circ$ ]	$A_b$ [kPa]	$B_b$ [kPa]	$n$ [-]
<b>D1</b>	3070	$90^\circ$	2500	3500	150
<b>PC10_2D_L5</b>	122	$90^\circ$	200	300	200

The result of the comparison between the outputs of the genetic algorithm and the solutions obtained using geotechnical softwares Flac 2D and RS2 is shown in Figures 5 and 6.

The output of the geotechnical analyses are given in red and are considered the target to be achieved by the genetic algorithm.

Axial force, bending moment and rotations of the lining are supposed to be known from the monitoring system in 12 points evenly spaced every  $30^\circ$  along the circular cross section of the lining itself.

Axial force and moment can be measured by means of pressure sensors embedded inside the concrete lining at (minimum) two different depths; a minimum total of 24 pressure sensors are therefore needed in every ring section.

The algorithm starts from the data provided by the user and shown in Table 3, uses the ground thrust shape functions presented in equations (3) to (6), calculates the loads acting from the ground to the lining, solves a simple finite element model of the lining without ground under self-equilibrated external loads coming from the ground, obtains axial force, N, bending moment, M, and rotation, R, diagrams of the lining, compares them with the known values from the monitoring system in 12 points, tries to minimize the difference between the calculated and the measured values of N, M and R.

The individual of the population that obtains the best mark through a weighted sum of the differences is considered to be the optimum solution.

In figure 4 and 5 the first two diagrams on the top show the comparison between the radial and the tangential loads exchanged between the ground and the lining in the complete FEM simulation (red) and calculated by the algorithm (cyan).

The following three diagrams on the left show the comparison between N, M and R obtained with the genetic algorithm (cyan) against the one given by the softwares and considered the target (red). On the right the error in % is shown.

Generally a very good accordance is achieved on the actions and on the axial force (errors almost always  $< 5\%$ ), whereas bigger mistakes are related to the calculation of rotations (up to  $20\%$ ) and bending moment up to  $100\%$ ). These very evident differences are due to the fact that bending actions were in all cases much smaller than axial actions, therefore the total deformation energy is related for its bigger portion to axial actions. Ovalization, and therefore rotations, are also due to the combination of axial and bending actions. They are not simply related to bending moment as it happens on straight beams. Therefore a big relative error on bending moment can still lead to a correct evaluation of the deformed shape of the lining (rotations) as most of the deformation is due to the variation of axial force.

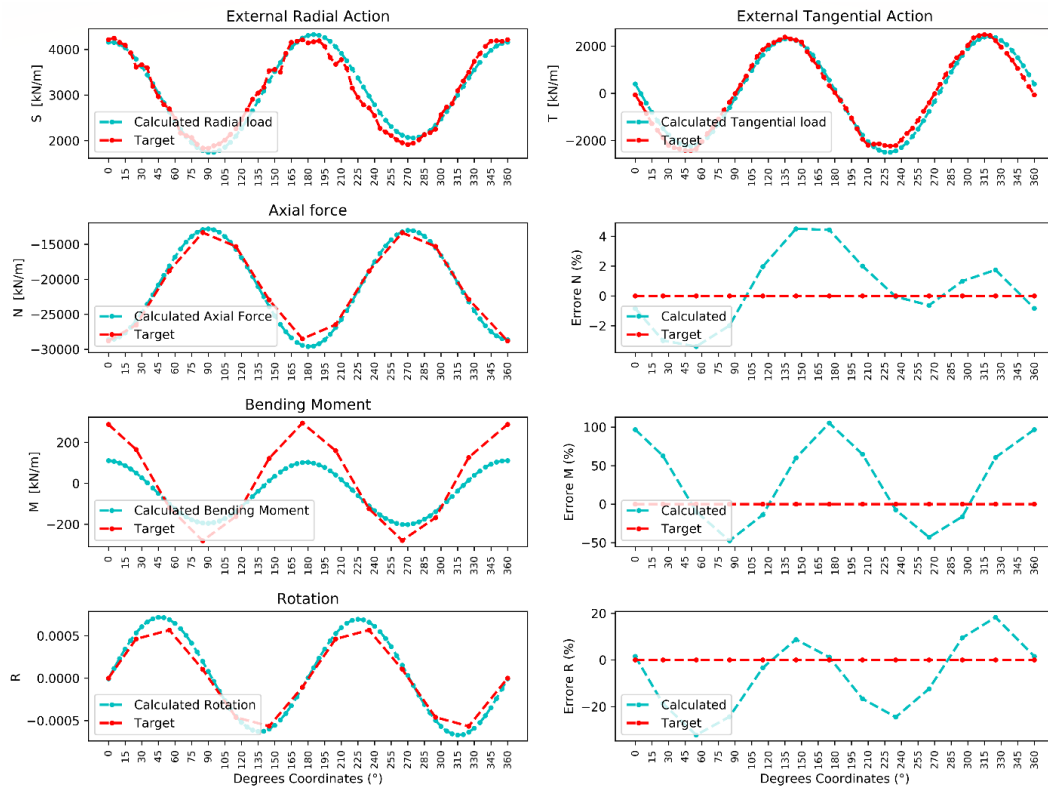


Figure 5. Tunnel D1 results comparison

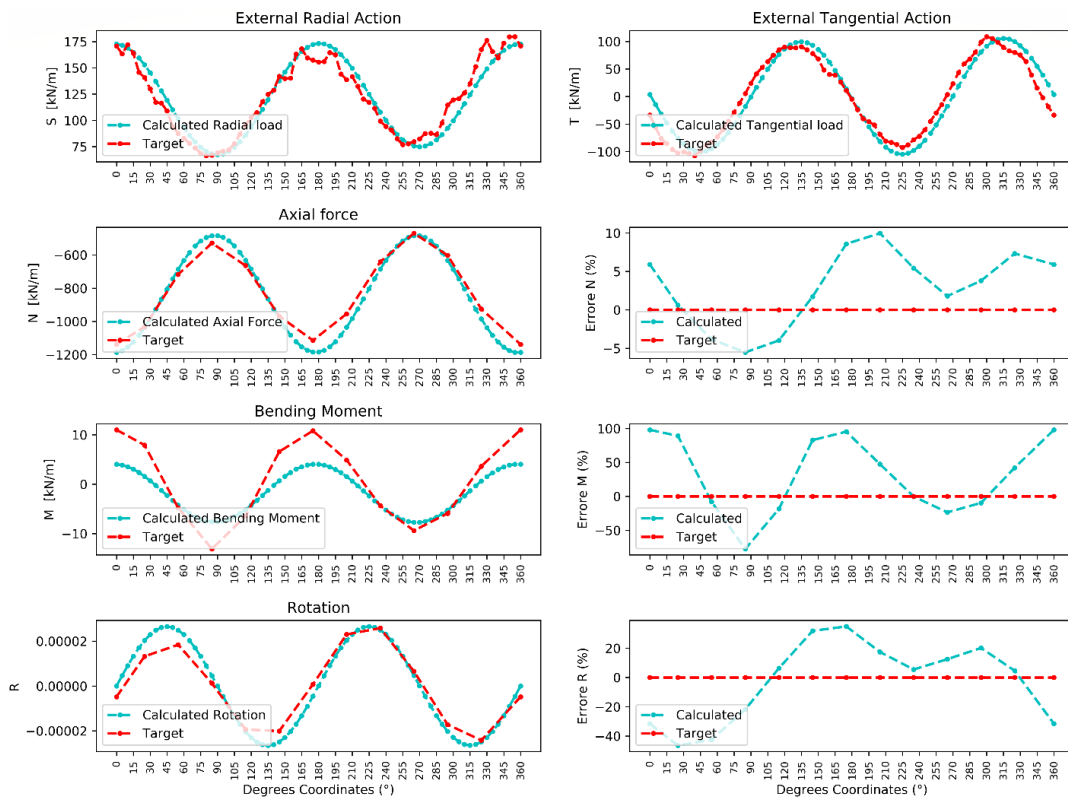


Figure 6. Tunnel PC10\_2D\_L5 results comparison

## 8. Conclusions and further developments

The same authors started two years ago the development of a genetic algorithm able to provide an interpretation to tunnel monitoring data. The first step was the definition of the quantities to be measured by the monitoring system and the development of the algorithm itself.

The present paper describes the second step of the process that is the test of the algorithm on a set of possible tunnels numerically modelled with well-known research softwares. This first set of test was performed considering simple elastic analyses with three construction phases and a wide range of possible soils and tunnel configuration.

As a consequence of these tests, the genetic algorithm has been supplied with new shape functions proposed in this paper and it has demonstrated to be able to fit properly many different layouts of shallow and deep tunnels.

Nevertheless the research space of the solution is formed by regular loads that are coming from geotechnical elastic analyses, both on ground side and on concrete one. More advanced applications that take into consideration the plasticization of the soil (i.e. using Coulomb or Tresca failure criteria), the presence of friction interfaces between lining and ground and the non linearities of reinforced concrete can and should be developed.

The birth of plasticized zones in the ground around the tunnel and the effect of other non-linearities may lead to the necessity of modifying the shape functions introducing more irregular functions. Obviously, the convergence of the algorithm is going to face more problems when deeply non-linear conditions are targeted. A higher number of individuals in the population may be needed in such cases.

## References

- [1] D. Balageas, C.-P. Fritzen, A. Güemes: “Structural Health Monitoring” Wiley, ISBN: 9781905209019, 2006.
- [2] C. Boller, F.-K. Chang, Y. Fujino, “Encyclopedia of Structural Health Monitoring”, Wiley, ISBN: 978-0-470-05822-0, 2009.
- [3] G. Bertagnoli, M. Malavisi, G. Mancini, “Large Scale Monitoring System for Existing Structures and Infrastructures”, World Multidisciplinary Civil Engineering-Architecture-Urban Planning Symposium, WMCAUS 2019 (IOP Conference series: Materials science and Engineering – vol. 603 Section 5) Prague, 17–21 June 2019 pp. 1-11, 2020.
- [4] G. Bertagnoli, F. Marino, “Evaluation of internal actions in tunnel lining applying genetic algorithms to monitoring data”, 4th World Multidisciplinary Civil Engineering-Architecture-Urban Planning Symposium, WMCAUS 2019 (IOP Conference series: Materials science and Engineering – vol. 603 Section 5) Prague, 17–21 June 2019 pp. 1-11.
- [5] C. Anerdi, D. Gino, M. Malavisi, G. Bertagnoli, “A sensor for embedded stress measure of concrete: testing and material heterogeneity issues”. Proceedings of Italian Concrete Days 2018 (Lecture Notes in Civil Engineering Book 42), Lecco 13-16 June 2018, pp. 3-15, 2020.
- [6] G. Bertagnoli, L. Giordano, S. Mancini, “Design and optimization of skew reinforcement in concrete shells”, *Structural Concrete*, vol. 13 n. 4, pp. 248-258, 2012.
- [7] G. Bertagnoli, L. Giordano, S. Mancini, “Optimization of concrete shells using genetic algorithms” *ZAMM - Journal of Applied Mathematics and Mechanics / Zeitschrift für Angewandte Mathematik und Mechanik*, vol. 94 n. 1-2, pp. 43-54, 2014.
- [8] G. Bertagnoli, L. Giordano, S. Mancini, “A Metaheuristic Approach to Skew Reinforcement Optimization in Concrete Shells Under Multiple Loading Conditions”, *Structural Engineering International*, vol. 24 n. 2, pp. 201-210, 2014.
- [9] FLAC Version 8.0 User’s Guide, Itasca Consulting Group, Inc. Minneapolis, USA, 2019.
- [10] RS2 2019 User’s Manual, Rocscience, Toronto, Canada, 2019.
- [11] ITACA (Italian Accelerometric Archive) [http://itaca.mi.ingv.it/ItacaNet\\_31/](http://itaca.mi.ingv.it/ItacaNet_31/) (last consulted on 05/05/2020).
- [12] Comité Européen de Normalisation, “EN 1998-1 Eurocode 8 - Design of structures for earthquake resistance Part 1: General rules, seismic actions and rules for buildings”, 2004